Performance of Nb Thin Films with Laser Induced Surface Corrugation

A. Badía–Majós[1], N. Lejeune [2], E. Martínez [1], L. Porta-Velilla [1], J. Frechilla [1], E. Fourneau [2], L. A. Angurel [1], G. F. de la Fuente [1], S. Marinkovic [2] and A. V. Silhanek [2]

[1] Instituto de Nanociencia y Materiales de Aragón
CSIC - Universidad de Zaragoza , Spain

[2] Experimental Physics of Nanostructured Materials
Q-MAT, CESAM, Université de Liège, Belgium

9th ICSM 2024

Navigation and tooltips work well with Acrobat reader, mainly in Full-screen mode

Motivation

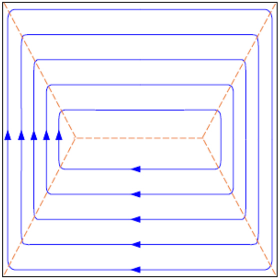

Surface modification (groove structure) to induce anisotropic current flow in SC films

$$\text{Sheet current: } \mathbf{K}(x,y) = \int \mathbf{J}(x,y)\,dz$$

Motivation

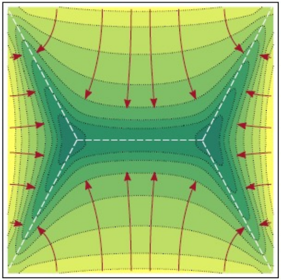

Surface modification (groove structure) to induce anisotropic magnetic flux penetration

$$..B_z(x,y) = \langle b_z(x,y) \rangle$$

OUTLINE

Background

Flux pinning by surface modification

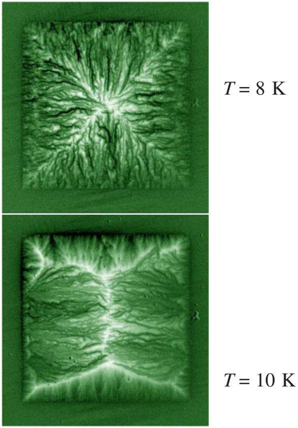

Flux penetration in patterned MgB_2 films

(as seen by MOI)

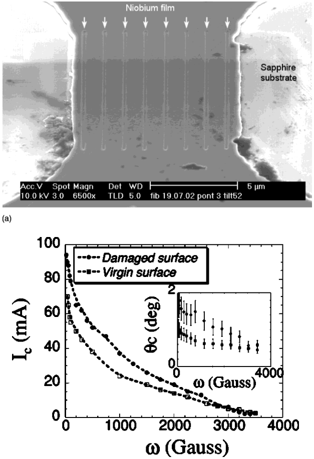

Critical current in corrugated Nb films

Surface modification by laser treatment

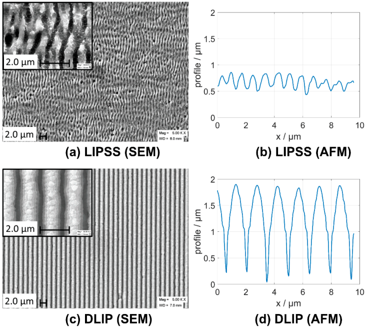

Laser **I**nduced **P**eriodic **S**urface **S**tructures

Direct **L**aser **I**nterference **P**atterns

- Surface treatments on steel

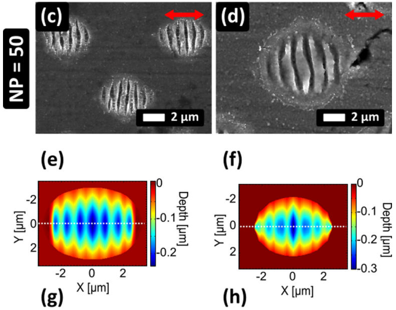

Experiment *vs* theory

- Laser pulses on steel

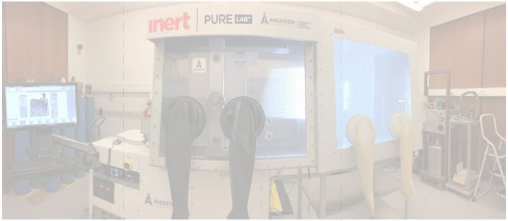

LIÈGE université

Materials and microstructure

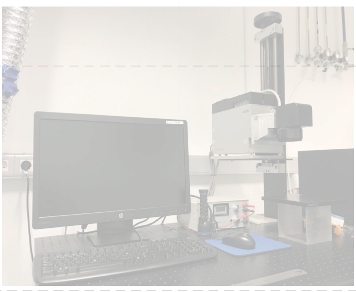

INMA
INSTITUTO DE NANOCIENCIA Y MATERIALES DE ARAGÓN

THIN FILM DEPOSITION

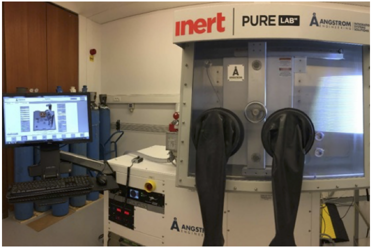

RF Sputtering..

- .Nb. films of thicknesses $d = 100, 200$ nm
- Deposited on Si substrates

$+$ PVD protective 7 nm layer of Al (or not)

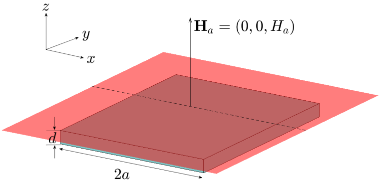

3×3 mm platelets laser-cut..

$$\zeta = \frac{d}{2a} < 10^{-4}$$

Pristine films

- TEM on untreated samples

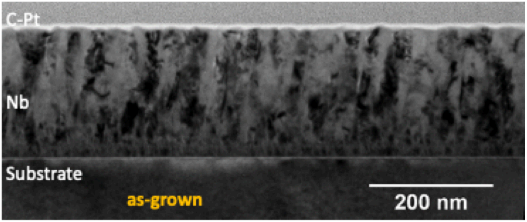

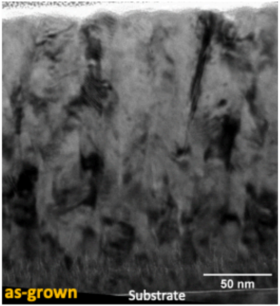

Nb films are polycrystalline, with very small grains (20-30 nm), display columnar growth, and smaller grain size close to the substrate (SiO_2)

Laser nanostructuring

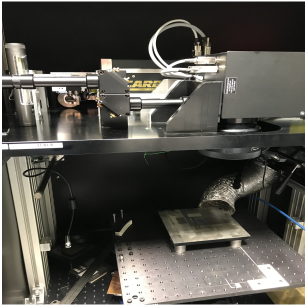

Step – by – step optimization process

1. – Double – pulses in fixed position
2. – Laser – scanning speed
3. – Line overlapping

Yb:YAG / 3H (Light Conversion)

Property	Value
Pulse duration τ_p	238 fs
Wavelength λ	343 nm
Pulse repetion f_{rep}	20 kHz
Spot	Elliptical $a \times b = 21 \times 34 \mu m^2$

Laser nanostructuring: energy per pulse(I)

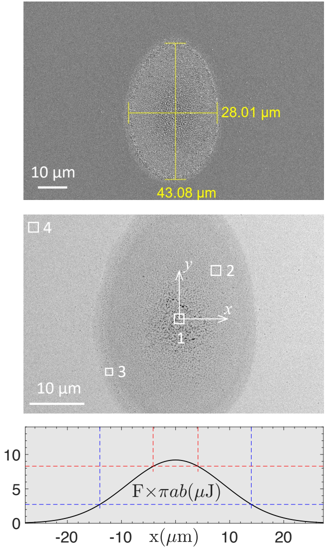

$E_{\mathrm{p}} = 4.6\mu\,\mathrm{J}$ per pulse

Label	O	Al	Si	Nb
1	5.5	0.8	28.8	64.8
2	7.1	-	10.4	82.5
3	8.7	4.2	3.8	83.4
4	4.6	8.6	3.4	83.3

Atomic %

LASER NANOSTRUCTURING: ENERGY PER PULSE (II)

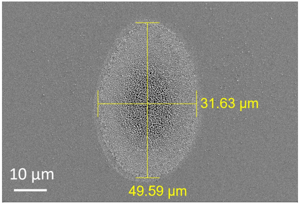

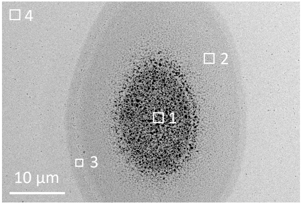

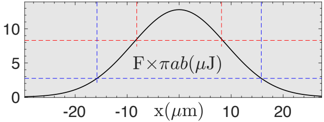

$E_\mathrm{p} = 6.4\mu\,\mathrm{J}$ per pulse

Label	O	Al	Si	Nb
1	4.3	–	59.6	36.1
2	6.2	–	11.7	82.1
3	10.3	2.0	4.5	83.2
4	5.1	8.5	3.4	83.0

Atomic %

LASER NANOSTRUCTURING (SCANNING MODE)

- Optimization of scanning speed and overlapping for given power

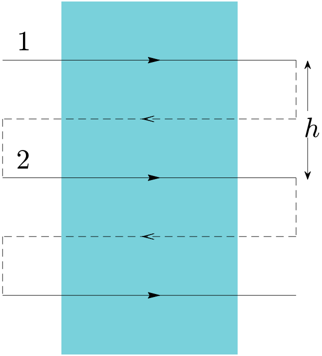

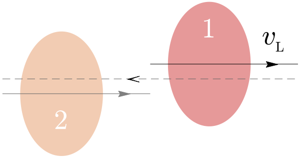

Laser nanostructuring (scanning speed and hatching)

- Optimization ($d = 200$ nm; Nb2 $\rightarrow$ Nb2L in air)

$\Rightarrow$ $E_\mathrm{p} = 3.0\,\mu\,\mathrm{J}$, $v_\mathrm{L} = 125\,\mathrm{mm/s}$, hatching $= 10\,\mu\mathrm{m}$

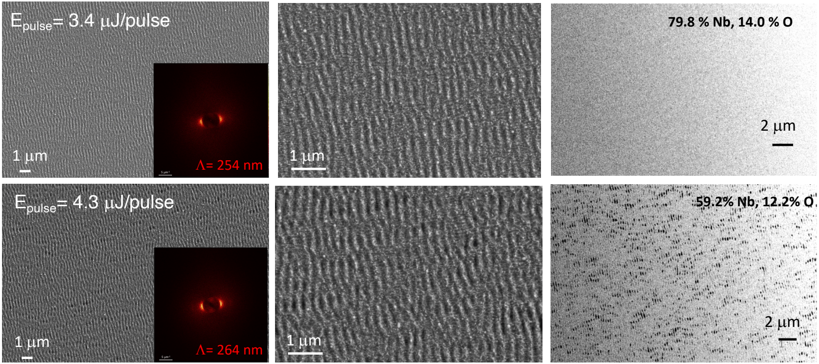

- Optimization ($d = 200$ nm; Nb2 $\rightarrow$ Nb2L in Ar)

$\Rightarrow$ $E_\mathrm{p} = 3.98\,\mu\,\mathrm{J}$ $v_\mathrm{L} = 125\,\mathrm{mm/s}$, hatching $= 10\,\mu\mathrm{m}$

Patterned films: topography (I)

- TEM on lamellae extracted from laser-treated samples in Ar

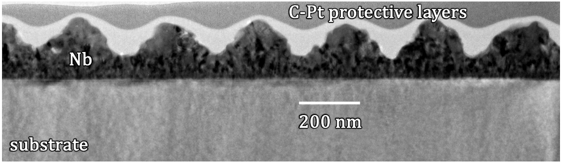

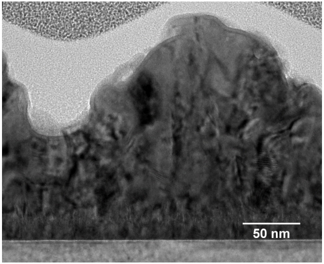

Images exhibit some changes in the film, i.e.: increased number of deffects in some grains (dislocations, rotations. . .). This happens mainly at the “valleys”.

PATTERNED FILMS: TOPOGRAPHY (II)

- Additional topographical information (AFM)

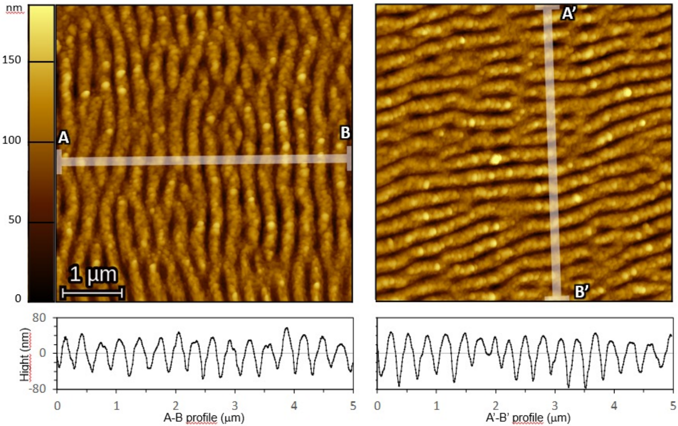

PATTERNED FILMS: FEASIBILITY

- Pattern design "à la carte"

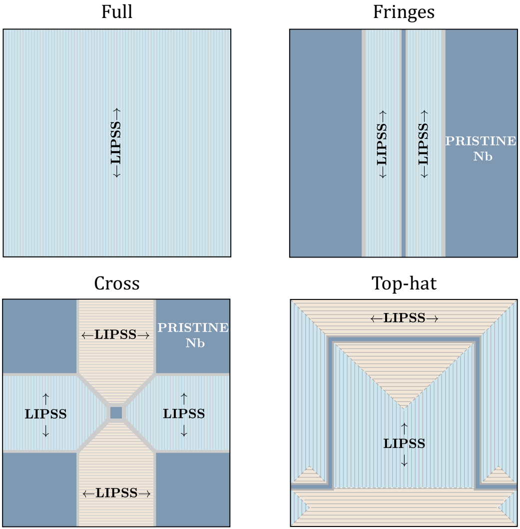

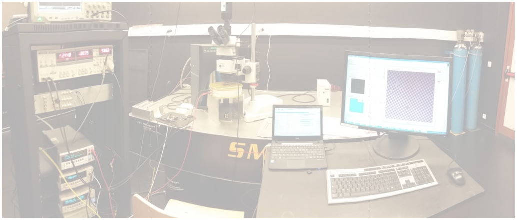

LIÈGE université

Physical properties

INMA
INSTITUTO DE NANOCIENCIA Y MATERIALES DE ARAGÓN

VOLUME MAGNETIC RESPONSE: T_c

- Low field diamagnetic response ($\mu_0 h_{AC} = 0.01$mT, $f = 10$Hz)

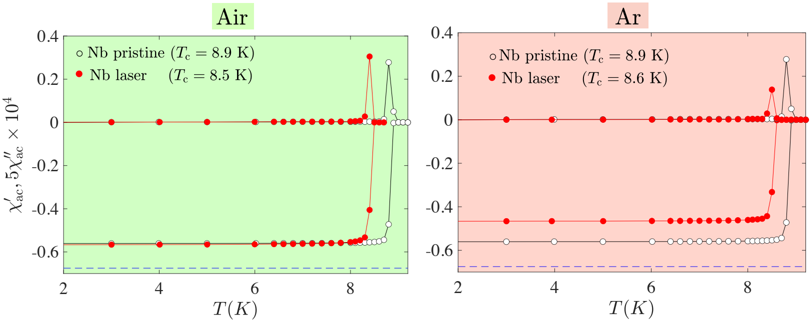

VOLUME MAGNETIC RESPONSE: SC FRACTIONS

- Pristine and laser patterned areas together in one sample (cross)

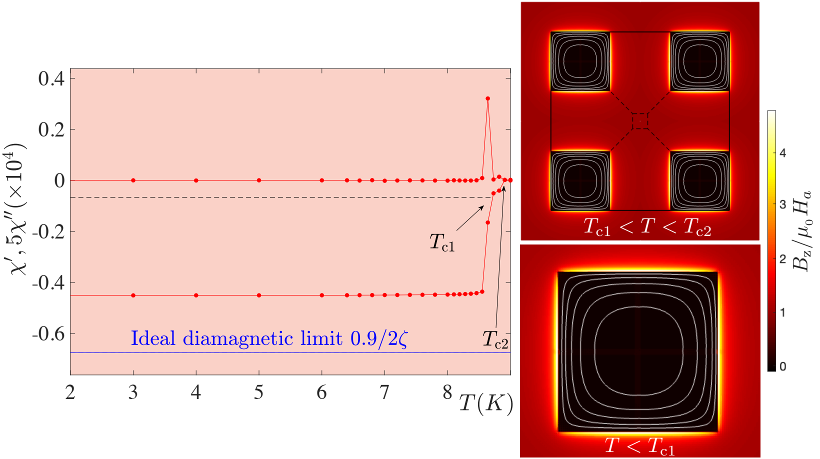

Low temperature magnetic instabilities

- Full patterned samples more prone to Low-T instabilities

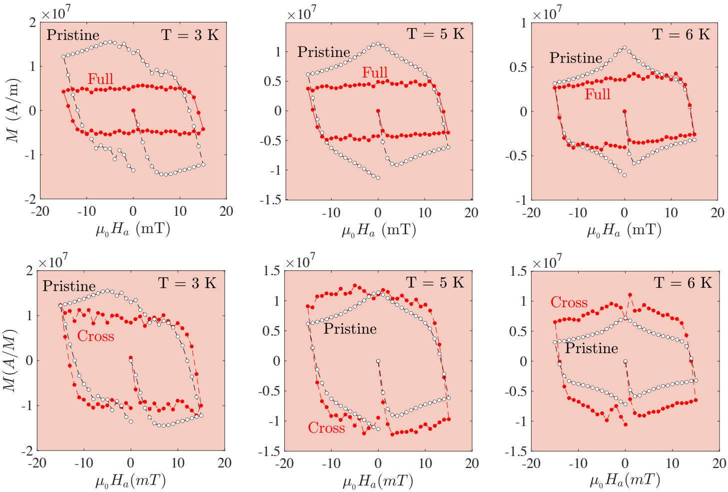

HIGH FIELD REVERSAL

- Overall irreversibility predominance, i.e.: $J_c(H)$, changes at high fields.

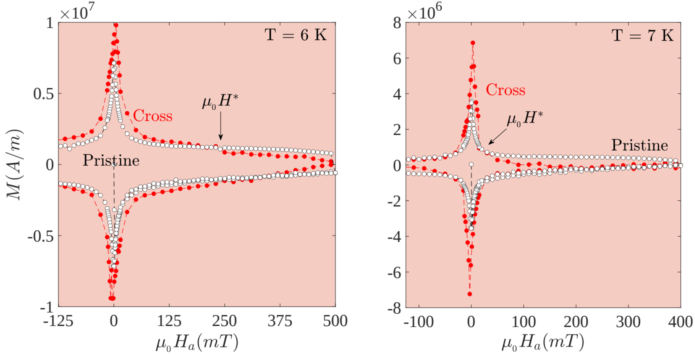

DC RESISTIVITY (I)

- *Anisotropic* resistive behavior ($H_a = 0, I_{\rm dc} = 100\mu$A) ..

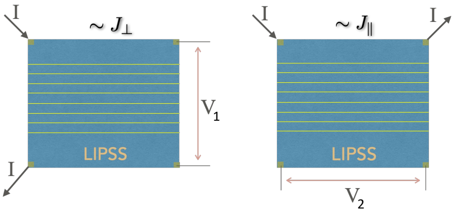

$$R_1 \equiv \frac{V_1}{I} \quad ; \quad R_2 \equiv \frac{V_2}{I}$$

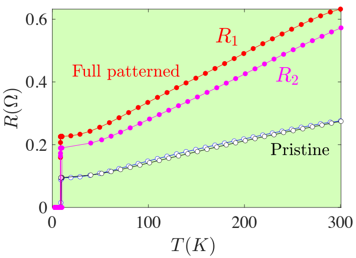

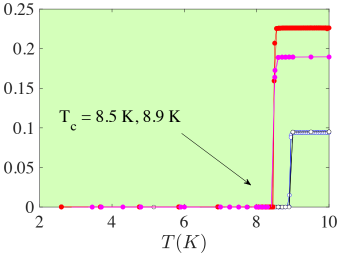

DC RESISTIVITY (II)

- *Anisotropic* resistive behavior: $R(H_a, T, I_{\rm dc} = 4.5\text{mA})$

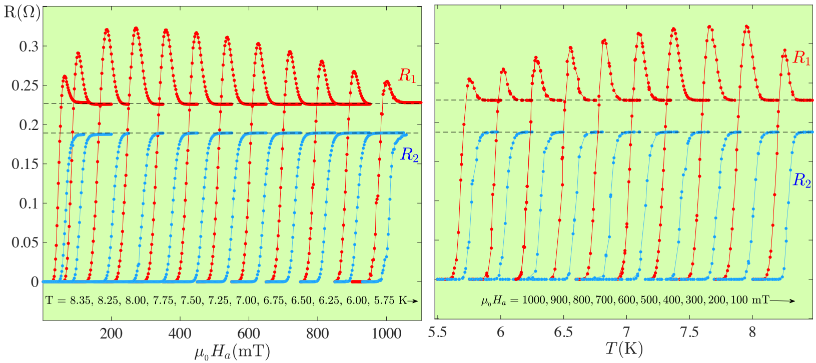

DC RESISTIVITY (III)

- *Anisotropic* resistive behavior: analysis ..

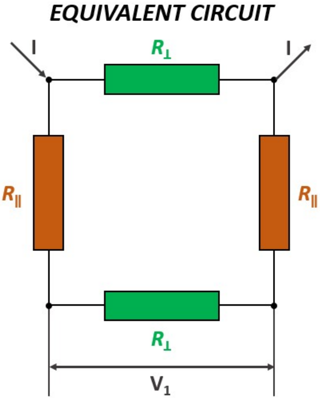

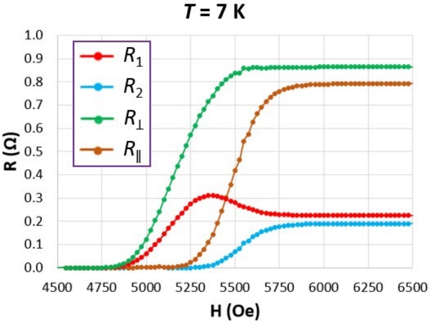

$$R_\perp = 2R_1 + 2\sqrt{R_1 R_2}$$

$$R_\parallel = 2R_2 + 2\sqrt{R_1 R_2}$$

Magnetic response (local)

LIPSS on Nb film

MOI flux profile

$J_{cy} = 2J_{cx}$ (Kim) ..

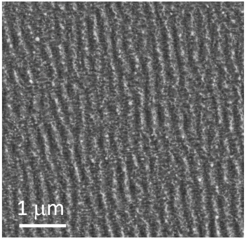

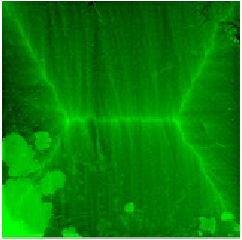

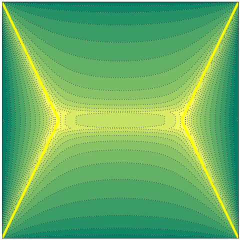

Magnetic response (local)

- *Magnetic flux avalanches* at $T = 0.51T_c$

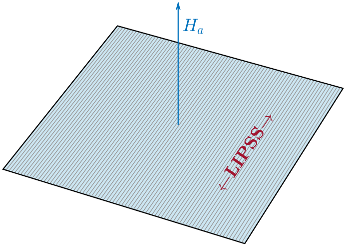

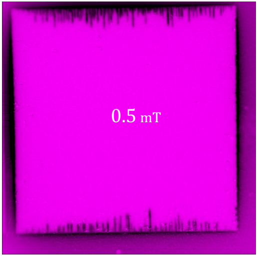

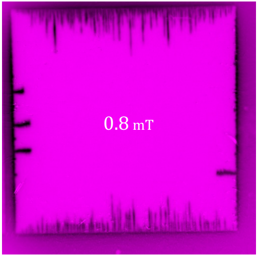

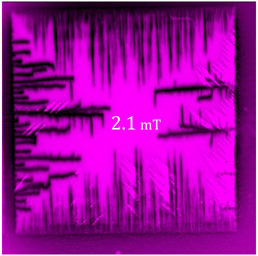

Local critical current density

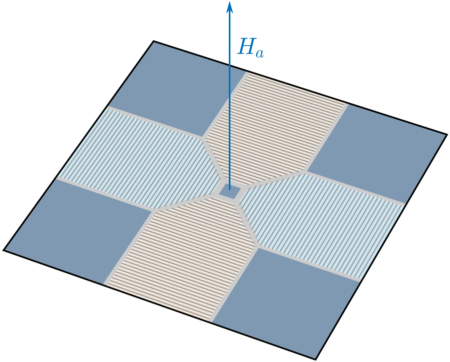

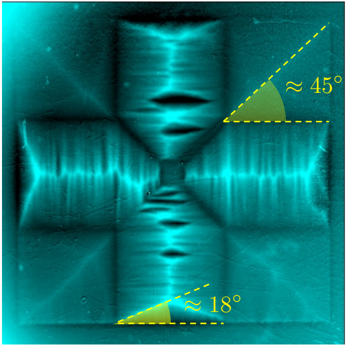

$$J_{c_\perp}/J_{c_\parallel} = \tan\vartheta \approx 1.0 \quad \text{(in pristine Nb)}$$

$$J_{c_\perp}/J_{c_\parallel} = \tan\vartheta \approx 0.32 \quad \text{(in LIPSS pattern)}$$

Local conductance at room temperature (cAFM)

- LIPSS topography vs. local surface resistance

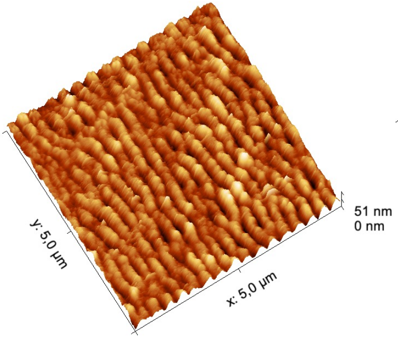

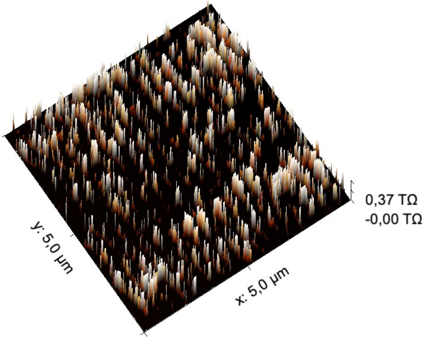

Local conductance at room temperature

- LIPSS topography vs. local surface resistance

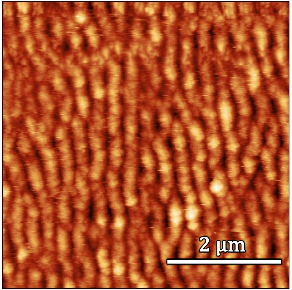

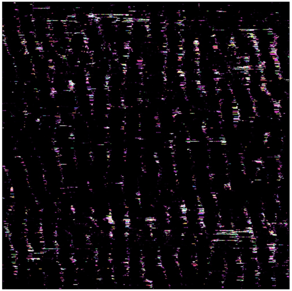

Local conductance at room temperature

- LIPSS topography vs. local surface resistance

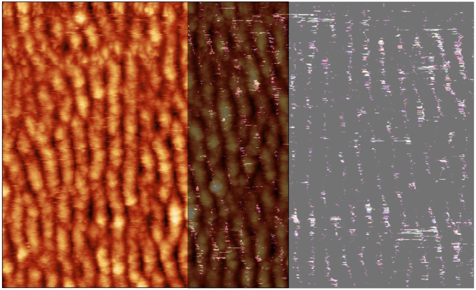

Local conductance at room temperature

- LIPSS topography vs. local surface resistance

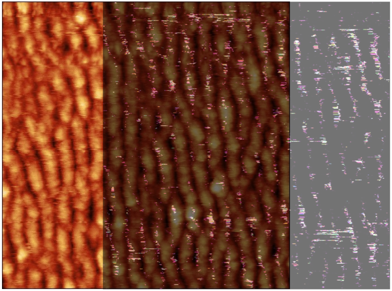

LOCAL CONDUCTANCE AT ROOM TEMPERATURE

- LIPSS topography vs. local surface resistance

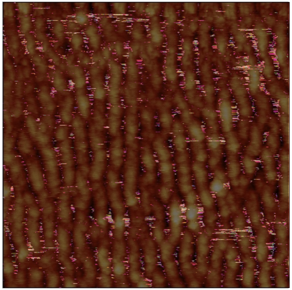

Interpretation of results

Min $\frac{1}{2}\sum_{i,j}\xi_{i,\mathrm{n}+1}M^x_{ij}\,\xi_{j,\mathrm{n}+1} - \sum_{i,j}\xi_{i,\mathrm{n}}M^x_{ij}\,\xi_{j,\mathrm{n}+1}$

$+\ \frac{1}{2}\sum_{i,j}\psi_{i,\mathrm{n}+1}M^y_{ij}\,\psi_{j,\mathrm{n}+1} - \sum_{i,j}\psi_{i,\mathrm{n}}M^y_{ij}\,\psi_{j,\mathrm{n}+1}$

$+\ \mu_0\sum_i\xi_{i,\mathrm{n}+1}(h_{x0,\mathrm{n}+1}-h_{x0,\mathrm{n}})$

$+\ \mu_0\sum_i\psi_{i,\mathrm{n}+1}(h_{y0,\mathrm{n}+1}-h_{y0,\mathrm{n}})$

for $(1-h^2_{x,i})\xi_i^2+(1-h^2_{y,i})\psi_i^2-2h_{x,i}h_{y,i}\,\xi_i\psi_i\le j^2_{c\perp}$

and $h^2_{x,i}\,\xi_i^2+h^2_{y,i}\,\psi_i^2+2h_{x,i}h_{y,i}\,\xi_i\psi_i\le j^2_{c\parallel}$

$$M^x_{ij}=M^y_{ij}\equiv 1+2\left[\min\{i,j\}\right]$$
$$M^x_{ii}=M^y_{ii}\equiv 2\left(\frac{1}{4}+i-1\right)$$

Isothermal Critical State Modelling in thin films

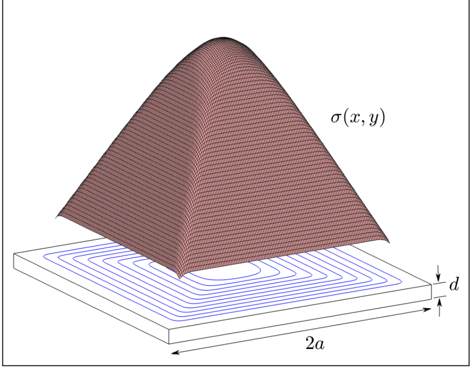

$$\mathbf{K}(x,y) = \int_{-d/2}^{d/2} \mathbf{J}\,(x,y,z)dz \equiv -\hat{\mathbf{z}}\times\nabla\sigma$$

$$m_z = \int_\Omega \sigma(x,y)dxdy$$

$$\mathcal{F}[\sigma_{\mathrm{n}+1}] \equiv \frac{1}{2}\iint_\Omega \left[\frac{\nabla\sigma_{\mathrm{n}+1}(\mathbf{r})\cdot\nabla\sigma_{\mathrm{n}+1}(\mathbf{r}')}{\|\mathbf{r}-\mathbf{r}'\|} - 2\frac{\nabla\sigma_{\mathrm{n}}(\mathbf{r})\cdot\nabla\sigma_{\mathrm{n}+1}(\mathbf{r}')}{\|\mathbf{r}-\mathbf{r}'\|}\right] d\mathbf{r}\,d\mathbf{r}'$$
$$+4\pi\left(H_z^{\mathrm{a,n+1}} - H_z^{\mathrm{a,n}}\right)\int_\Omega \sigma_{\mathrm{n}+1}(\mathbf{r})\,d\mathbf{r} + \mathit{dissipation}$$

Global Anisotropic Critical State Model

- *Anisotropic Bean model* ($J_{cx} = J_{cy}/\gamma$)

$$M_s = J_{cx}a\left[\frac{(2\gamma-1)(1-\gamma)}{2\gamma} + \frac{3\gamma^2-3\gamma+1}{3\gamma}\right] \longrightarrow \boxed{M_s(\gamma=2)} = 1.25\,\frac{J_c a}{3} = \boxed{1.25 M_s(\gamma=1)}$$

- *Anisotropic Kim model* in square platelet $\left(J_{cx}^2 + \frac{J_{cy}^2}{\gamma^2} \leq \frac{J_{c0}^2}{(1+H/H_0)^2}\right)$ ..

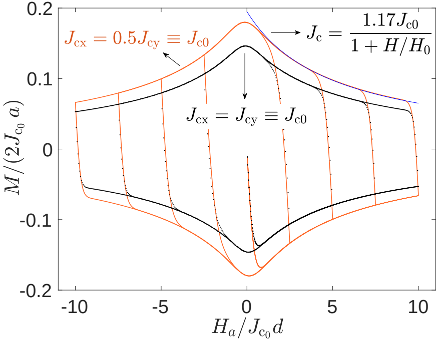

$$\boxed{\frac{M_s(\gamma=2)}{M_s(\gamma=1)} \approx 1.23}$$

Inhomogeneous Anisotropic Critical State Model

- Local modification of J_c in multidomain architectures

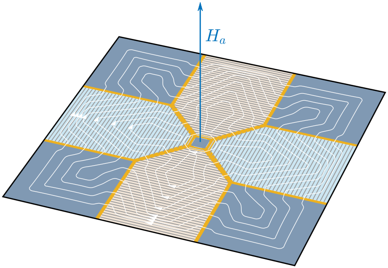

Simulated sheet current

for inhomogeneous $\mathbf{J}_c(\mathbf{r}, H_a)$ distribution

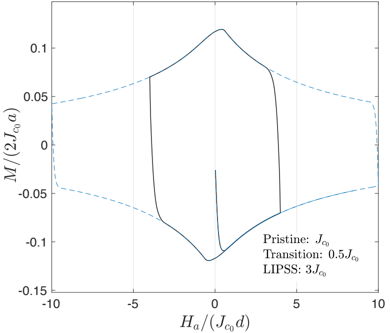

Simulated hysteresis loops

for the inhomogeneous $\mathbf{J}(\mathbf{r}, H_a)$ distribution

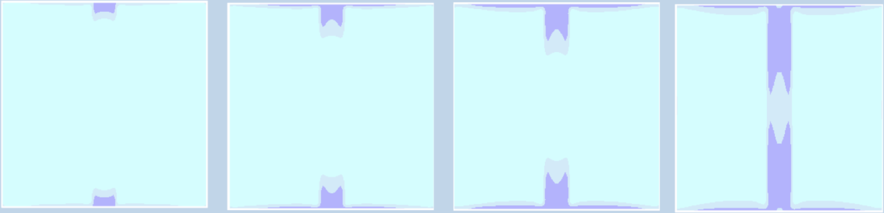

Prospect

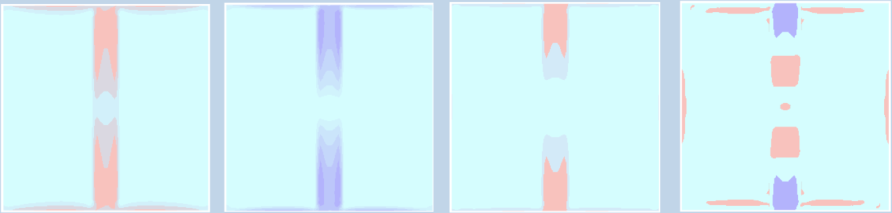

Conceptual challenge: magnetic flux pathway

- Magnetic flux channels in between protected domains

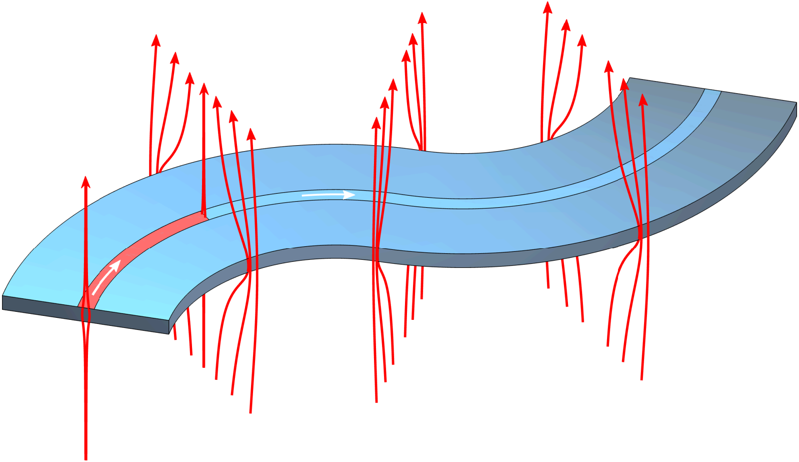

Conclusions

LASER NANOSTRUCTURED Nb THIN FILMS

Laser nanostructured Nb thin films

- Ultrashort laser pulses $\Rightarrow$ Nb films nanopatterning

($\tau_p = 238$ fs, $\lambda = 343$ nm $\rightarrow$ quasiperiodic surface ripples, $\Lambda \approx 250$nm)

LASER NANOSTRUCTURED Nb THIN FILMS

- Ultrashort laser pulses $\Rightarrow$ Nb films nanopatterning
($\tau_p = 238$ fs, $\lambda = 343$ nm $\rightarrow$ quasiperiodic surface ripples, $\Lambda \approx 250$nm)

- Process optimization (shallow grooves on thin Nb)
(Control parameters $\rightarrow$ laser $E_p, F_{rep}, v_{\mathrm{L}}$, polarization, atmosphere)

LASER NANOSTRUCTURED Nb THIN FILMS

- Ultrashort laser pulses $\Rightarrow$ Nb films nanopatterning
($\tau_p = 238$ fs, $\lambda = 343$ nm $\rightarrow$ quasiperiodic surface ripples, $\Lambda \approx 250$nm)
- Process optimization (shallow grooves on thin Nb)
(Control parameters $\rightarrow$ laser $E_p, F_{rep}, v_{\mathrm{L}}$, polarization, atmosphere)
- Superconducting parameters are modified anisotropically
($\Delta T_{\mathrm{c}}(\|, \perp), \Delta H_{\mathrm{c}_2}(\|, \perp), J_{\mathrm{c}}(\|, \perp)$ & modified pinning mechanisms)

LASER NANOSTRUCTURED Nb THIN FILMS

- Ultrashort laser pulses $\Rightarrow$ Nb films nanopatterning
($\tau_p = 238$ fs, $\lambda = 343$ nm $\rightarrow$ quasiperiodic surface ripples, $\Lambda \approx 250$nm)

- Process optimization (shallow grooves on thin Nb)
(Control parameters $\rightarrow$ laser $E_p, F_{rep}, v_{\mathrm{L}}$, polarization, atmosphere)

- Superconducting parameters are modified anisotropically
($\Delta T_{\mathrm{c}}(\|, \perp), \Delta H_{\mathrm{c_2}}(\|, \perp), J_{\mathrm{c}}(\|, \perp)$ & modified pinning mechanisms)

- Flux avalanche channeling at lower temperatures
(Competition: anisotropic J_{c} *vs.* groove flux channeling)

LASER NANOSTRUCTURED Nb THIN FILMS

- Ultrashort laser pulses $\Rightarrow$ Nb films nanopatterning
  ($\tau_p = 238$ fs, $\lambda = 343$ nm $\rightarrow$ quasiperiodic surface ripples, $\Lambda \approx 250$nm)
- Process optimization (shallow grooves on thin Nb)
  (Control parameters $\rightarrow$ laser $E_p, F_{rep}, v_{\mathrm{L}}$, polarization, atmosphere)
- Superconducting parameters are modified anisotropically
  ($\Delta T_{\mathrm{c}}(\parallel, \perp), \Delta H_{\mathrm{c}_2}(\parallel, \perp), J_{\mathrm{c}}(\parallel, \perp)$ & modified pinning mechanisms)
- Flux avalanche channeling at lower temperatures
  (Competition: anisotropic J_{c} *vs.* groove flux channeling)
- “Multi-domain configurations” promote directional flux penetration
  (Prospective application: magnetic flux channeling)

Many thanks for your attention !

The authors gratefully acknowledge the financial support from:
• Spanish MCIN/AEI/10.13039/501100011033 (project PID2020-113034RB-I00)
• Gobierno de Aragón (research group T54_23R)
• Belgian FNRS Fonds de la Recherche Scientifique
• Hi-Scale COST action (CA19108)

The authors also would like to acknowledge the use of *Servicio General de Apoyo a la Investigación-SAI*, Universidad de Zaragoza.

“Many thanks to all group members”

Laser, Energy & Advanced Materials (LEMA)
Institute of Nanoscience and Materials of Aragón
Zaragoza (Spain)

Experimental Physics of Nanostructured Materials
Q-MAT, CESAM, Université de Liège
Liège (Belgium)

Supplementary material

Simplest solution: Bean's model (CSM)

- Infinite slab $|x| \leq w$ in parallel field $(0, 0, \mu_0 H_a)$ ..

$$\frac{dB}{dx} = \pm\mu_0 J_c(B) \quad \text{or} \quad 0$$

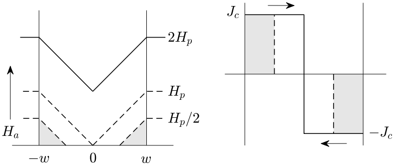

$$M_V = \frac{\langle B \rangle}{\mu_0} - H_a$$

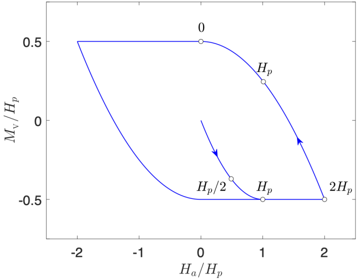

- Provides physical interpretation
- May be used to .characterise. the sample $\Delta M_V = J_c w$

GENERALISING BEAN'S MODEL

- The evolutionary statement

$$\texttt{Minimize}\quad \mathcal{C} \equiv \frac{1}{2\mu_0}\int_{\mathbb{R}^3} \|\mathbf{B}_{\mathrm{n}+1} - \mathbf{B}_{\mathrm{n}}\|^2 + \Delta t \int_{\Omega} \mathcal{P}[J]$$

$$\Updownarrow$$

$$\mathcal{C}[\mathbf{J}_{\mathrm{n}+1}] = \int_V d^3\mathbf{r} \int_V d^3\mathbf{r}' \left[\frac{\mathbf{J}_{\mathrm{n}+1}(\mathbf{r}) \cdot \mathbf{J}_{\mathrm{n}+1}(\mathbf{r}')}{\|\mathbf{r} - \mathbf{r}'\|} - 2\frac{\mathbf{J}_{\mathrm{n}}(\mathbf{r}) \cdot \mathbf{J}_{\mathrm{n}+1}(\mathbf{r}')}{\|\mathbf{r} - \mathbf{r}'\|}\right]$$

self-interaction

$$+ \frac{8\pi}{\mu_0}\int_V d^3\mathbf{r}\,(\mathbf{A}_{\mathrm{e,n}+1} - \mathbf{A}_{\mathrm{e,n}}) \cdot \mathbf{J}_{\mathrm{n}+1} + \frac{4\pi\Delta t}{\mu_0}\int_V d^3\mathbf{r}\,\mathcal{P}(J_{\|,\mathrm{n}+1}, J_{\perp,\mathrm{n}+1})$$

interaction with EM sources

interaction with thermal modes

- Circuital interpretation (FEM)

$$\mathcal{C} \equiv \mathcal{C}_{\mathrm{JJ}} + \mathcal{C}_{\mathrm{J0}} + \mathcal{C}_{\mathrm{JS}} + \Delta t\, \mathcal{W}_{\mathrm{JE}} = \left[\frac{1}{2}\langle \mathtt{J} | \mathtt{m} | \mathtt{J} \rangle - \langle \mathbf{J}^{\vee} | \mathtt{m} | \mathbf{J} \rangle + \langle \Delta\psi_{\mathrm{S}} | \mathtt{J} \rangle + \Delta t\, \mathcal{W}_{\mathrm{JE}}\right]$$

$\mathcal{C}_{\mathrm{JJ}}$: self energy of the evolutionary circulating currents

$\mathcal{C}_{\mathrm{J0}}$: interaction energy of the evolutionary currents with a “frozen” distribution

$\mathcal{C}_{\mathrm{JS}}$: interaction energy of the evolutionary currents with the magnetic source

$\Delta t\, \mathcal{W}_{\mathrm{JE}}$: energy related to the entropy production due to dissipative mechanisms

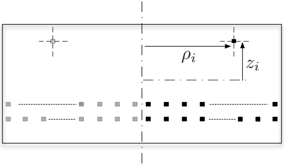

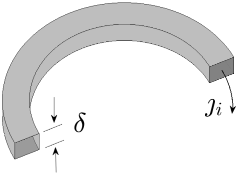

Mikheenko's approximation

Sheet current approximation